Renewable Energy 220 (2024) 119422

Contents lists available at ScienceDirect

Renewable Energy

journal homepage: www.elsevier.com/locate/renene

Characterisation of soiling on glass surfaces and their impact on optical and solar photovoltaic performance

Tarik Alkharusi [a], Gan Huang [a,b], Christos N. Markides [a,*]

[a] Clean Energy Processes (CEP) Laboratory, Department of Chemical Engineering, Imperial College London, London, UK
[b] Institute of Microstructure Technology, Karlsruhe Institute of Technology, Karlsruhe, Germany

ARTICLE INFO

Keywords:
Dust particles
Optical losses
Photovoltaic
Soiling
Solar energy
Transmittance

ABSTRACT

Photovoltaic (PV) module soiling, i.e., the accumulation of soil deposits on the surface of a PV module, directly affects the amount of solar energy received by the PV cells in that module and has also been suggested as a mechanism that can give rise to additional heating, leading to significant power generation losses or even physical degradation, damage and lifetime reduction. Investigations of PV soiling are challenging and limited. We present results from an extensive outdoor experimental testing campaign of soiling, apply detailed characterisation techniques, and consider the resulting losses. Soil from sixty low-iron glass coupons was collected at various tilt angles over a study period of 12 months to capture monthly, seasonal and annual variations. The coupons were exposed to outdoor conditions to mimic the upper surface of PV modules. Transmittance measurements showed that the horizontal coupons experienced the highest degree of soiling. The horizontal wet-season, dry-season and full-year samples experienced a relative transmittance decrease of 62 %, 66 %, and 60 %, respectively, which corresponds to a predicted relative decrease of 62 %, 66 %, and 60 % in electrical power generation. An analysis of the soiling matter using an X-ray diffractometer and a scanning electron microscope showed the presence of particulate matter with diameters <10 μm (PM10), which was the most prevalent in the studied region. The findings of this study lay the groundwork for research into soiling mitigation practices.

1. Introduction

Solar photovoltaic (PV) technology has been proliferating in recent decades, driven by the global trend towards clean and cost-effective energy [1]. The total cumulative installed PV capacity is expected to reach about 1 TW by the end of 2023 and over 2 TW by 2025 [2]. The International Renewable Energy Agency (IRENA) recently reported that solar PV costs have declined by 82 % over the last decade [3], and in 2020, the International Energy Agency (IEA) declared solar PV to be the cheapest electricity source [4]. Despite the widespread implementation of solar PV systems, the electrical efficiency of commercial PV modules is limited to 10–25 % [5], with the majority (at least ~70–80 %) of the incoming solar radiation lost in the form of waste heat, which has a detrimental impact on the electrical efficiency of these systems [6]. Multi-faceted efforts are being made to remove and/or utilise the heat generated within PV cells, either by direct module [7] cooling or by integration into hybrid PV-thermal (PV-T) collectors [8] that can be deployed in domestic applications [9], for urban cooling/heating [10,11], and even desalination [12,13,14]. In all such PV-based technologies, however, sustaining performance close to the theoretical or manufacturer-stated levels is often challenging due to issues related to climatic parameters [15]. Solar irradiance, relative humidity, wind speed, rainfall, and the tilt angle of a module are key factors that affect the performance of PV-based systems [16–19], while depending on the location, these factors can also significantly impact the formation of soiling, which refers to the settling and accumulation of any airborne materials on the sun-facing surface of these syetms. This reduces the amount of solar energy received by the solar cells [20], resulting in power generation losses due to the lower transmittance, but has also been suggested as a mechanism that can give rise to additional heating, leading to further power losses [21,22]. Furthermore, the formation of localised soiling spots can create hot spot regions that may lead to a greater rate of cell degradation over a system's lifetime [7,23,24].

PV efficiency is directly impacted in regions with high air pollution and dust concentration, such as Africa, the Middle East, India, and China [3,25]. A study by Bergin et al. [26] estimated atmospheric particulate matter (PM) and dust accumulation can cause up to a 25 % reduction in solar energy production in these regions. Anthropogenic air pollution is the main contributor in India and China, while in the Arabian Peninsula

* Corresponding author.
E-mail address: c.markides@imperial.ac.uk (C.N. Markides).

https://doi.org/10.1016/j.renene.2023.119422
Received 19 May 2023; Received in revised form 7 September 2023; Accepted 5 October 2023
Available online 6 October 2023

Nomenclature

Abbreviations

CF	capacity factor
PV	photovoltaic
UV–Vis	ultraviolet–visible spectroscopy
XRD	X-ray diffractometer
SEM	scanning electronic microscope
PM10	particulate matter of diameter <10 μm
PM2.5	particulate matter of diameter <2.5 μm

Symbols

J_0	dark saturation current (A/m^2)
$G_{AM1.5}$	incident solar irradiance (W/m^2 nm)
q	elementary charge (C)
K	Boltzmann constant (W/m^2 K^4)

Greek symbols

τ_{drop}	transmittance decrease of soiled glass coupon relative to clean glass coupon (%)
τ_x	transmittance of soiled glass coupon (-)
τ_r	transmittance of reference (clean) low-iron glass coupon (-)
τ	spectral transmittance
β_{PV}	PV cell temperature coefficient (1/K)
ε	emissivity (-)

and Northern Africa, pollution is primarily caused by natural resources (i.e., sandstorms). In 2018, China alone accounted for more than 50 % of the installed PV capacity globally [27]. Researchers reported that aerosols reduce solar irradiance by up to 35 % in China [28]. Given that Africa, the Middle East, India, and China will account for 60 % of the global PV capacity by 2050 and are among the regions with the highest global solar radiation availability, as shown in Fig. 1, soiling losses are a concerning challenge. Li et al. [29] calculated the global average PV capacity factors (CFs), by converting the maximum available radiation on optimally tilted modules into electricity. These CFs correspond to the actual annual electricity generation divided by the theoretical maximum electricity generation. They found that the CFs ranged from 0.20 to 0.30 in most solar-resource-abundant regions, as shown in Fig. 2. The west coast of South America and Western China record high CFs beyond 0.25, while the CF in the rest of the world is below 0.20. Desert areas and highly polluted areas experience lower CFs than would be theoretically possible due to low precipitation, high dust deposition and atmospheric aerosols, as shown in Fig. 2. They concluded that Northern Africa and the Middle East CFs are below 0.1 which is 60 % lower than those of clean modules due to dust concentration. The Middle East and North Africa are known to have a significantly higher amount of natural atmospheric dust (>50 μg/m^3) compared to other regions, making them one of the worst soiling zones in the world [30,31]. It has been reported that PV systems in a desert climate can perhaps suffer power losses of 1 % per day [23,29]. Even in Southern Europe, known for its favourable weather conditions, a recent study reveals that Spain experiences a soiling rate of 0.14 % per day [32].

Adinoyi et al. [33] found that dust accumulation on the surface of a PV module over six months in Saudi Arabia reduced the module power output by 50 %. Chanchangi et al. [34] reported a yield loss of 78 % in Nigeria for PV modules over 12 months without cleaning. They also reported the highest optical losses of 88 % for horizontal tilt angle [35]. Enaganti et al. [36] exposed low-iron glass samples to natural soiling conditions in India for 120 days without cleaning and revealed a 17 % decrease in transmittance. Furthermore, Abdolzadeh et al. [37] designed wooden boxes with glasses embedded at different tilt angles to capture dust deposition in different directions. Results demonstrated that dust deposition reduced the output PV power by 15 % during the one-year study period. After ten weeks of being exposed to outdoor conditions, a 21 % reduction in the power output was experimentally examined in Tehran, Iran [38]. Elminir et al. [39] developed an experimental set-up involving 100 glass samples with different tilt angles. They evaluated their transmittance over a period of seven months, taking into consideration thunderstorms that occurred during the study period. They show that there is an inverse correlation between the tilt angle and the deposition density, which was also reported by Ref. [40]. They reported a module efficiency reduction of 17 % per month at an angle of 45° facing south in Mania, Egypt. It was also reported that the transmittance decrease reached 53 % at the end of the study period of 210 days for glass samples installed at 0°.

A desalination plant in Abu Dhabi, UAE, powered with evacuated tube collectors suffered a 60 % decrease in overall plant production due to solar-collector soiling. They concluded that weekly cleaning was important to mitigate any losses due to soiling [41]. Ullah et al. [42,43] found that the projected power losses in Lahore, Pakistan for PV modules were up to 10 % and 40 % due to light and heavy soiling, respectively. Mazumder et al. [44] reported experimentally that dust depositions as low as 10 mg/cm^2 can cause a 90 % power reduction. Dehshiri et al. [45] found that the annual reduction in electricity production due to the soiling effect in the southwestern part of Iran can reach up to 80 %. It has been reported that a 1 MWe PV solar power plant in the semi-arid climate of Morocco can experience annual power losses of 0.24 % per day due to soiling [46]. Not only the amount of dust accumulated, but also the physical and chemical composition of the accumulated soiling, can have an impact on the efficiency of the PV modules [47,48]. A comprehensive understanding of the soiling effects

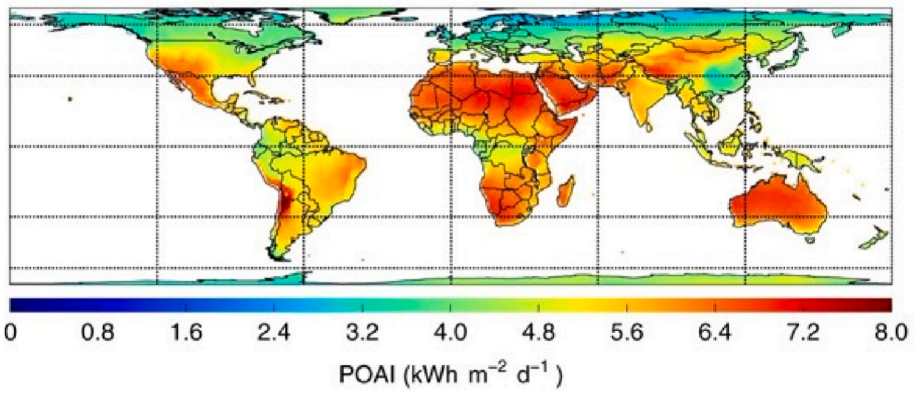

Fig. 1. Global data for surface point of array irradiance as adapted from Li et al. [27]. The Middle East, Northern and Southern Africa and Western China have irradiance above 7 kWh/m^2 per day, while Europe and Canada have irradiance below 4 kWh/m^2 per day.

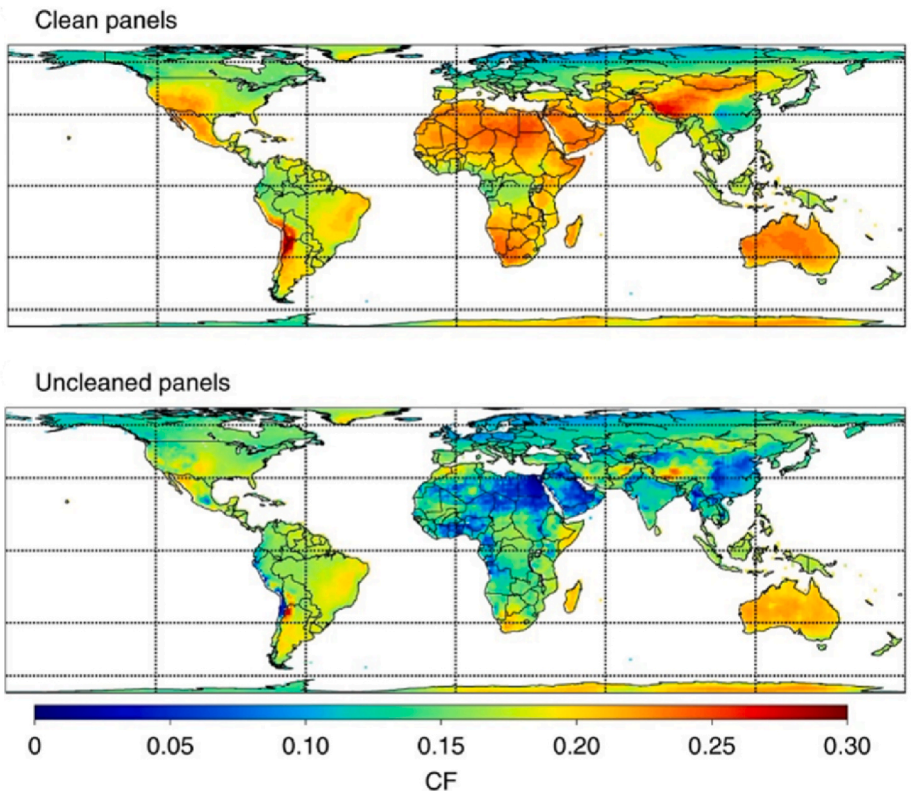

Fig. 2. Global data for capacity factor (CF) for clean and uncleaned PV modules. Average CF in the Middle East, Northern and Southern Africa, and Western China is above 0.20 and can decrease by 150 % for soiled/uncleaned modules, visible in the difference between subfigures without cleaning manually or naturally (i.e., rain) [27]. For example, clean modules operate with CF values in the range 0.2-0.25 in the Middle East, which drops to 0.05-0.1 under soiled conditions.

of a region is needed before installing a PV system [49,50], as each location is unique and accurately measuring soiling losses is challenging [51]. In 2023, global losses from PV soiling are projected to increase to ~7 %, resulting in a staggering revenue loss of approximately 7 billion euros worldwide [52].

Countries across the globe have tremendous potential for solar energy utilisation using PV technologies. However, estimating the energy yield from real PV installations remains challenging due to an over/underestimation of soiling losses. Soiling losses strongly depend on particle size, shape and their associated spectra which significantly impact PV performance. The novelty of the present work is in the comprehensive full-year assessment of soiling losses using detailed optical and material characterisation techniques that translate to PV module power deterioration. The reported findings aim to enrich current knowledge of PV soiling, to improve estimates of associated losses and to improve the forecasting of PV system yields.

2. Methods

In this section, the procedures that were followed to gather and analyse the soiling samples are outlined. Section 2.1 presents the data collection approach. In Section 2.2, the data processing steps are

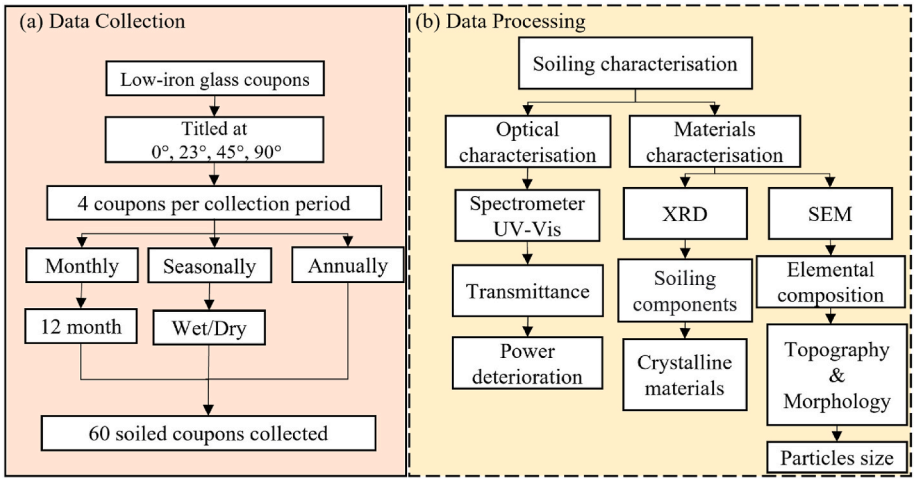

Fig. 3. Flow chart showing the methodology adopted to collect the soiling data (left) followed by the data processing and analysis undertaken to analyse the collected data (right).

described, which include the equipment employed and analysis methods. The entire method applied in this work to gather and analyse the soiling data is summarised in Fig. 3. The weather data for the assigned location is presented in Section 2.3.

2.1. Soiling-sample data collection

The soiling coupons used were collected from a soiling data station, assembled and fixed on a residential rooftop in Muscat, Oman's capital city. Table 1 provides site exposure data and shows the solar energy potential in the selected region. The experiment used low-iron glass coupons measuring (50 mm × 50 mm × 4 mm). The low-iron glass was chosen primarily because of its widespread use within the solar industry for encapsulating the top layer of a PV module [53]. Different methods were adopted throughout the literature to assess soiling losses in a wide range of applications, and the use of glass coupons to assess soiling losses is an established approach [54–56]. Thus, the effect of soiling was examined. Understanding the effect of soiling over the variation in climate conditions across the studied period is important.

The data were collected in order to capture annual variations in the soiling at a monthly resolution over a one-year study period from the 1st of January 2021 to the 31st of December 2021. The seasonal and annual variations were examined separately during the study period. As Oman experiences two main seasons, the study period is classified into two main seasonal periods: the Wet season, running from January through to April, and the Dry season, which runs from June through to September. May and October are considered "changeover months" [57].

To consider the impact of the tilt angle on the soiling deposition variations, the glass coupons were installed at four different tilt angles: 0°, 23°, 45° and 90° from the horizontal. This resulted in 60 collected glass coupons in total: 4 glass coupons collected at the end of each month, 4 glass coupons at the end of each season, and 4 glass coupons at the end of the whole year.

The glass coupons were installed in a soiling station: a wall-mounted set-up consisting of three 3D-printed jigs and each jig was designed and printed with a slit to hold the glass coupon at the designed tilt angle. The design of each 3D-printed jig used in the soiling data station with different tilt angles is shown in Fig. 4.

At the end of each month, the monthly soiled glass coupons were removed and replaced with clean low-iron glass coupons. The same process was done for all the Wet-season, Dry-season and full-year glass coupons at the end of their data-collection period, as all glass coupons were installed on the first day of the collection period and removed after the last. All collected soiling samples were transferred from the soiling station to the Clean Energy Processes (CEP) Laboratory at Imperial College London for experimental investigation.

2.2. Soiling sample analysis

Analysis was carried out on the soiling glass coupons collected to ascertain the optical losses due to soiling. This involved optical characterisation, utilising a UV–Vis spectrophotometer, and spectral analysis, using an X-ray diffractometer and a scanning electron microscope (SEM). The results of the soiling characterisation are separated into two parts: optical characterisation and material characterisation.

Table 1
Site information obtained from the global solar atlas (GSA), 2022 [56].

Coordinates	23.594°	North
	58.427°	East
Direct normal irradiation	1950	kWh/m^2
Global horizontal irradiation	2180	kWh/m^2
Diffuse horizontal irradiation	860	kWh/m^2
Global tilted irradiation at the optimum angle	2370	kWh/m^2
Optimum tilt angle of PV modules	26/180	°
Average air temperature	29	°C
Terrain elevation above sea level	23	M

The initial analysis involved the inspection of the optical losses, (i.e., transmittance), by employing a spectrophotometer. Table 2 outlines the parameter configuration used in this experimental analysis. A Shimadzu UV-2600 spectrophotometer was used with a wavelength range from 200 to 1100 nm to accommodate the response of different PV modules which can range from ultraviolet (UV) to near-infrared (NIR) light. A clean low-iron glass was used to establish a referenced transmittance value. All of the soiled samples were then compared to this reference value to assess their optical losses. A collected soiled glass coupon was compared to a clean one to demonstrate the visual impact of soiling as shown in Fig. 5.

Since the UV-2600 spectrophotometer used in this present work had a restricted line-scanning size, all of the soiled glass coupons were placed at the same position within the scanning chamber to guarantee that all soiled coupons were scanned in the same region. The relative transmission decrease of each soiled coupon was measured against the referenced clean glass coupon with a decrease in transmittance characterised by Ref. [59]:

$$\Delta\tau_{\text{drop}} = 1 - \frac{\tau_x}{\tau_{\text{r}}}, \tag{1}$$

where $\Delta\tau_{\text{drop}}$ is the relative decrease in transmittance of a soiled sample, τ_x is the measured soiled coupon transmittance, and τ_{r} is the referenced transmittance of a clean glass coupon.

2.2.1. Material characterisation

PV soiling refers to a variety of particles such as snow, dirt, dust, leaves, or pollen, etc., that accumulate on PV module surfaces [60]. These particles can interact with (i.e., reflect, scatter and absorb) the incident sunlight, thus affecting performance in a way that depends on their size and shape. The composition of the soiling material varies widely by location [61], making it critical to investigate soiling properties such as size distribution, shape and composition in order to assess local soiling losses. An X-ray diffractometer (XRD) and a scanning electron microscope (SEM) were used to investigate the soiling mineral. Based on the fact that all soiling data was collected from the exact location, we have constructed the assumption that all glass coupons contain similar soiling matter. Thus, the glass coupons chosen for material characterisation were horizontal glass coupons for the wet and dry seasons and the full year. This assumption will be validated based on the XRD and SEM findings.

2.3. Weather data

PV soiling refers to the accumulation of dust, snow, dirt, and other particles on the upper surface of a solar module, which can reduce their efficiency and generate less power. Weather condition plays a significant role in determining the soiling rate of a solar module. For example, the soiling rate may be lower in wet regions due to the regular cleaning effect of rain compared to dry areas where soiling particles can accumulate rapidly on the upper surface of a solar module. Thus, it is essential to look at the specific weather conditions of the location of this study in order to understand the causes of dust accumulation over the collected glass coupons. The studied area is considered a semi-desert region that is dry and hot with dusty winds that receive little precipitation ranging from 5 to 15 mm per year. The metrological data of the studied location from the 1st of January 2021 to the 31st of December 2021 is shown in Fig. 6 [62]. Oman is a coastal area that offers variations in temperature owing to ocean currents with high summer temperatures and minimal yearly rainfall. In general, Oman is affected by different atmospheric conditions (the Mediterranean, Central Asia, the tropical maritime of the Indian Ocean) that produce significant variations in rainfall in different parts of the country.

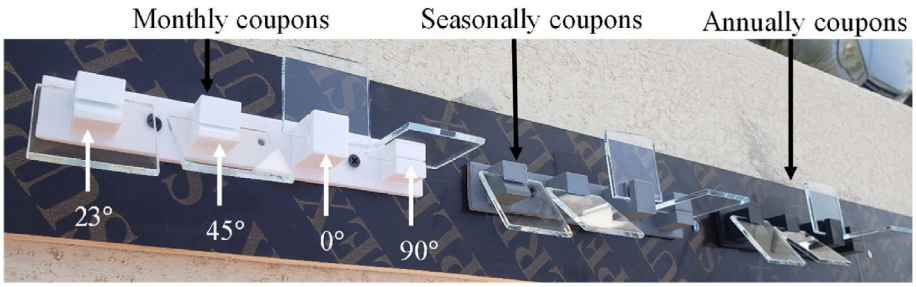

Fig. 4. Photograph showing the design of the soiling station used to collect the soiling samples throughout the experiment. The station consists of three 3D-printed jigs for each collection period fixed on a wooden plate structure for stability and mounted to the wall.

Table 2
Parameters of the Shimadzu UV-2600 spectrophotometer.

Photometric system	Double-beam optics
Photometric mode	Transmittance
Detector	Photomultiplier R-928
Light source	50 W halogen lamp, deuterium lamp
Measurement range	200–1200 nm
Resolution	0.1 nm
Photometric range	0–100000 %
Photometric accuracy	±0.3 %
Photometric repeatability	±0.1 %
Scan mode	Single
Accumulation time	0.1 s
Detector unit	Direct
Slit width	2 nm
Sample interval	1 nm
Noise level	Maximum 0.00003 Abs

Fig. 5. Photographs showing the one-year horizontal sample at the end of the study period (left) alongside a clean glass coupon (right).

3. Results and discussion

The analysis first involved reporting the soiling station data in Section 3.1. The 60 soiled coupons collected during the study period were assessed and characterised optically in Section 3.2 and materially in Section 3.3 to understand the influence of soiling on the transmittance of collected samples. Section 3.4 presents the electrical power losses.

3.1. Soiling station

As can be seen in Fig. 7, the collected coupons demonstrate a significant variation in the soiling ratio across the seasonal and full-year samples. A closer inspection of the coupons in Fig. 7 indicates the significance of the influence of the tilt angle on the amount of soiled matter accrued over the glass surface. There is a strong negative correlation between the tilt angle (when tilting from horizontal to vertical) with the amount of dust accumulated. The horizontal coupons (those with a tilt angle of 0°) had the greatest level of soiling, while the vertical coupons (those with a tilt angle of 90°) had the lowest level of soiling. This could be possibly attributed to the fact that the wind, in conjunction with gravitational force, can reduce soiling particles over a tilted surface.

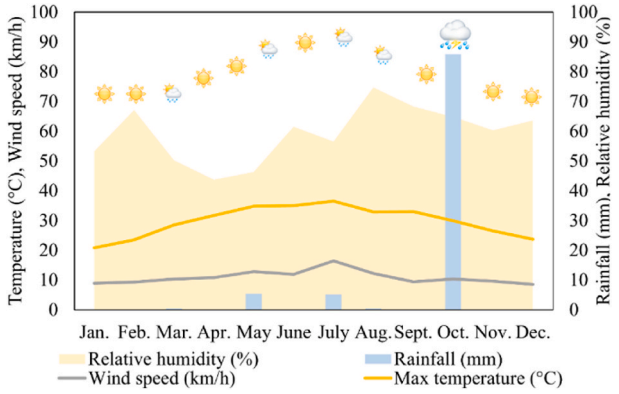

Fig. 6. Meteorological data for the year 2021 of the studied location, Muscat, was retrieved from the Directorate General of Meteorology, the Civil Aviation Authority of Oman [60].

However, solid visual evidence shows that the effect of wind-driven cleaning and gravity was insufficient to clean the surface, and other mitigation techniques are required for this region. The dry-season coupons have more sandy and powdery soiling formations, which resemble the studied area's environmental conditions, whilst cementation was visible mainly on the wet-season coupons due to the high moisture levels. This cementation effect enhances the adhesion between the soiling particles and the glass coupon surface which is not favoured in the PV installation areas because it can cause a significant reduction in power output. When a portion of a PV module is shaded with soiling depositions, it experiences a decrease in voltage and current, which can affect the system's overall performance. Therefore, PV systems are typically designed and installed in locations where they receive maximum sunlight exposure with minimal shading.

The most interesting results of the soiling patterns are reported in Fig. 8, which captures separate monthly exposure periods. First, the patterns in the dust visible in Fig. 8 confirm that soiling particles display heterogeneous morphology characteristics, leading to a multifarious spectrum of soiling patterns. Second, the environmental conditions and the choice of tilt angle impact the formation of accumulated dust significantly. Third, the results are well aligned with our assumption that a mitigation technique is needed to avoid excessive soiling and that a proper understanding of the soiling matter is essential to select the appropriate method to clean installed PV modules. Thirteen different soiling properties were examined indoors to study the effect of soiling properties on PV performance and concluded that each type of thirteen-soiling matter has different levels of light transmittance disturbance [63].

3.2. Optical transmittance reduction

The wet-season, dry-season and full-year coupons provide a general understanding of soiling losses in the studied region. By focusing on the decrease in glass transmittance as a representation of the light reaching

Fig. 7. Photographs showing twelve glass samples of collected soiled glass coupons for different seasons (wet and dry seasons) and for the whole year at four different tilt angles: 0°, 23°, 45° and 90° (the backgrounds of the photographs are pure black).

Fig. 8. Photographs showing sixteen samples of soiled glass coupons collected for the months of April, May, October and November, and at four orientations each. These months were selected to show the overall variation in dust depositions over the course of the persent (annual) investigation.

the solar cell and disregarding the thermophoresis effect, it is possible to estimate the power degradation by comparing a dirty glass coupon to a clean one. Thermophoresis is a phenomenon in which particles in a fluid move in response to a temperature gradient. Fig. 9 shows the decrease in measured transmittance of soiled glass coupons at the end of different seasonal and annual exposure periods.

The results in Fig. 9 show that the soiling impact varies depending on the tilt angle. A clear trend is visible across all three periods: the lower the tilt angle of the solar module to the horizontal, the lower the transmittance. Hence, the reduction in transmittance leads to a decrease in the amount of incident light reaching the solar cells, resulting in an overall decline in power output. We attribute this to an increase in the tilt angle causing large particles to roll off, as rolling is the dominant detachment process when drag forces are present with the support of the gravitational force. The relative transmittance decrease of the horizontal samples of the wet-season, dry-season and full-year coupons was 62 %, 66 %, and 60 %, respectively. In comparison, the vertical coupons showed a relative transmittance drop of 28 %, 11 % and 24 %, respectively. The average relative transmittance decrease across all tilt angles was 39 %, 45 % and 35 % for the wet, dry and one-year coupons, respectively. Overall, across the seasons, the maximum decrease was recorded during the dry season.

One noteworthy result acquired from full-year coupons was the significance of changes in environmental conditions: the larger-than-average rainfall during October 2021 of 94 mm is potentially responsible for the relative difference in transmittance reduction between full-year and seasonal glass coupons. The glass coupons subjected to natural soiling conditions across all tilt angles for one year had lower soiling deposition, with an average 35 % decline in transmittance compared to 39 % for the wet season and 45 % for the dry season, against a clean sample with a tested transmittance of 89 % over the measured wavelengths range of 350-1100 nm, with an averege transmittance of 91 % within the visible wavelength range [36,54,84]. The studied location, Muscat, Oman, received 94 mm of rain in 24 h on the 3rd of October 2021 due to cyclone activity [62], over 115 times the average October rainfall for Muscat of 0.8 mm and 110 % of the yearly average of 89.7 mm [64].

The October tropical cyclone goes some way to explaining the partial removal of soiling deposition over the collected glass coupon surfaces for the full-year sample compared with the seasonal sample. However, despite the unpredictable heavy rainfall during the cyclone, the observed difference in periods of expected rainfall levels showed that natural soiling removal was insufficient to notably clean the glass coupons. The results demonstrate that natural soiling removal methods, such as wind and rain, are inadequate to clean PV modules as there remains a significant relative transmittance decrease of 35 % for full-year-exposed coupons. Consistent with the literature [65,66], these data support the view that heavy rainfall can partially clean modules and could potentially reduce, but not eliminate, manual cleaning requirements. The variations in monthly transmittance across the entire study period are shown in Fig. 10.

Climatic parameters such as the ambient temperature, relative humidity, wind speed and rainfall, and the module's tilt angle are key factors that have an effect on the accumulation of soiling over the surface of the collected glass coupons. Several observations could explain this. First, the rainfall in the second week of March permitted soiling particles to accumulate more than similar environmental circumstances in January and February for the 0°, 23° and 45° coupons. Due to the light rainfall combined with the increased tilt angle, the vertical coupon (90°) in March was slightly cleaner than February's and January's coupons, as shown in Fig. 11.

Second, as reported in Refs. [67–70], air-moisture level plays a significant role in the formation of soiling. Rain incidents affected the April glass coupons by increasing the adhesion of soiling particles to the surface of the coupons. This influence was noticeable even with the vertically-titled glass coupons, as seen in Fig. 10. An actual soiling pattern for the vertical coupons is shown in Fig. 11, where soiling patterns are distributed similarly, except for the April coupon, which is clustered in thick layers. The soiling particles cemented to the surface as this process resulted in dust glueing after becoming damp due to the rainfall [71]. The presence of water forms capillary bridges between the dust particles and the surface, promoting soiling-particle accumulation over the surface [63,72]. Cleaning the cemented soiling growth, an example of which is shown in Fig. 8, requires a large amount of water and physical effort to retain the optical performance of the glass, resulting in additional costs. Even though an average rainfall of 5.4 mm was experienced in May compared to minor rain in April, the rain only minimised the soiling accumulation over the tilted surfaces. The lowest relative average monthly transmittance decrease was observed during May and October; changeover months that experience seasonal change and unstable climate conditions. This seasonal weather changeover affects the coupons regardless of the tilt angle position, notable in a reduction in the average relative transmittance of 28 % and 25 %.

The presence of water can expedite soiling formation and enhance the adhesion force between soiling particles and the glass coupon surface. In the absence of water during dry season conditions (i.e., August), soiling particles have a greater tendency to roll or slide off the glass coupon surface compared to wet weather conditions (i.e., April), as shown in Fig. 12b and a, respectively. Olympus digital microscope (BX41-LED) was deployed to examine these glass coupons. As shown in

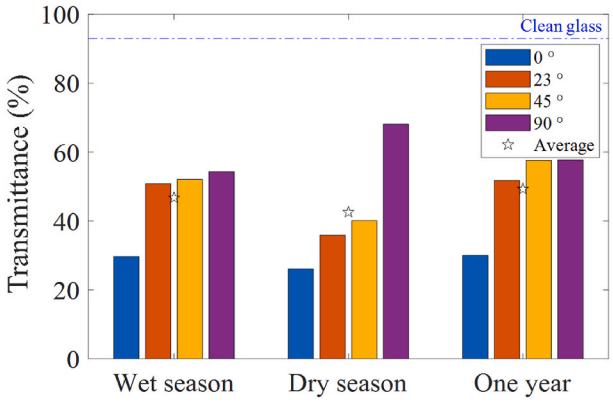

Fig. 9. Transmittance of soiled coupons collected at the end of the wet season, dry season, and over a full year, for four different tilt angles as well as the average of each period. The transmittance of a clean glass coupon is shown with a dotted blue horizontal line for reference.

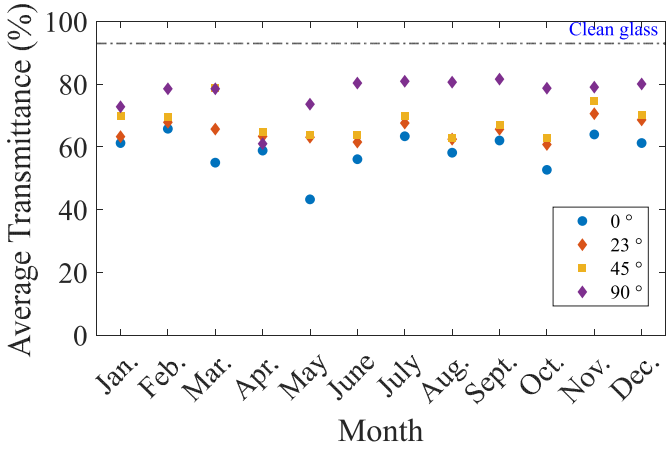

Fig. 10. Average transmittance for coupons exposed for one month through the entire study period for four different tilt angles represented by the four different colours in the plot. The transmittance of a clean glass coupon is shown with a dotted blue horizontal line.

Fig. 11. Vertical soiled coupons for January, February, March and April. The measured average transmittance was 77 %, 82 %, 82 %, and 61 %, respectively.

Fig. 10, the August vertical tilt coupon transmittance shows a 31 % improvement with measured transmittance at 80 % compared to 61 % for April vertical tilt coupon.

3.3. Soiling matter characterisation

A strong relationship between soiling characterisation and transmittance reduction has been reported in the literature. The soiling particle size has a negative correlation with dust accumulation: larger particles (>10 μm) under low relative humidity have lower transmittance losses, and fine particles (<10 μm) have higher transmittance losses [73–75]. Our results have shown that small dust particles are challenging to remove and thus influence the reduction in PV efficiency. The XRD and SEM methodologies are used to classify the soiling material captured during the studied period. All glass coupons are collected to examine the soiling variation losses across seasons (wet and dry) and a full-year cycle. In order to identify the worst possible scenario, horizontal glass coupons were selected. This selection was based on the assumption that all 60 coupons were gathered from the same area, thus sharing similar soiling matter.

Variations across all three samples were initially shown visually in Fig. 7. The soiling particles over the dry sample surface appeared dustier with fine-rounded powdery formations similar to dust particles that generally occur in the desert environment. In contrast, large soiling particles gradually scour from the surface with rainfall. Small particles remain cemented to the surface, forming the pattern shown on the wet-season coupons. This can be attributed to the air moisture level during the wet season compared to dry weather. Both seasons' soiling patterns are observable on the full-year coupon, as shown in Fig. 13.

Together, these results support our initial assumption that the selected coupons are sufficient to make conclusions for the whole collected soiling data. In addition, the full-year sample has a unique pattern due to an accumulation period of 365 days with exposure to various weather conditions during the exposure time, as shown in Fig. 6. The results of the full-year sample can also be used to provide the overall transmittance reduction corresponding to the energy yield losses, assuming that the PV surface is not cleaned for one full year.

Fig. 13. Illustration of soiling distributions for the one-year horizontal sample demonstrating a similar pattern to the patterns captured separately during wet and dry seasons.

3.3.1. X-ray diffraction test results

XRD analysis determines a material's crystalline structure, chemical composition, and physical characteristics. Initially, a clean low-iron glass was examined to ensure that all diffracted rays were due to the soiling substance and not due to the low-iron glass compositions. Fig. 14 reveals that all captured diffracted beams are formed from the soiling substance. The list of peak intensities is here compared to the latest

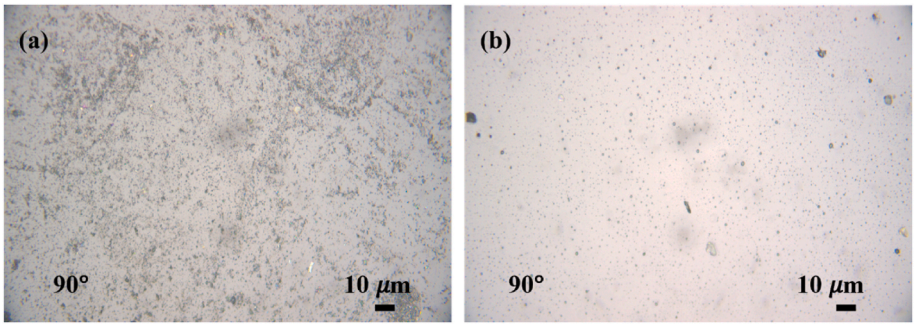

Fig. 12. Optical microscope images at 50 × magnification were taken of vertical tilt glass coupons from two different collection periods: (a) a wet season month (April) and (b) a dry season month (August), as shown in the photographs. The presence of water facilitates the adhesion of soiling particles to the glass coupon surface, resulting in particle cementation.

version (PDF-4+ 2022) reference patterns retrieved from the International Centre for Diffraction Data (ICDD) [76]. Fig. 15 compares the three horizontal coupons used for this examination to analyse the fluctuation of peak patterns and determine the soiling-specific chemistry and atomic compositions. It is interesting to compare the three samples showing relative peak patterns with different intensities, resulting in sharper peaks in the dry season compared with the wet season. These findings agree with the visual inspection of these coupons shown in Fig. 7 of Section 3.1. In contrast, the full-year sample still captures both peak patterns, which aligns with the assumption that all collected coupons share similar soiling matter.

According to the XRD findings, the full-year horizontal soiled coupon has a variety of minerals such as silicon dioxide, calcium carbonate, calcium magnesium carbonate, titanium dioxide, iron carbide, and aluminium silicate. Fig. 14 shows a snapshot of XRD peaks analysis which determines the chemical compounds of soiling particles. The chemical compounds reported by XRD are mainly derived from natural resources such as sand, limestone, and marble, followed slightly by minerals output of industrial activities. The dominant mineral found is silicon dioxide, the chemical compound of silica (quartz) generally found in nature as sand, which makes sense given the environmental conditions of the studied area. There are similarities between the minerals expressed in this study and those described by Refs. [77,78]. Silica is considered one of the major cementing agents [79,80] and is the primary mineral found in the collected soiling samples, which explains the cementation effect under the tested weather conditions.

3.3.2. Scanning electron-microscope test results

The air quality index measured at the experimental site (Muscat) showed a higher concentration of PM10 and PM2.5. The SEM images of Fig. 16 show the diversity in particle sizes and shapes. Image data is processed based on the frequency of soiling minerals across dry-season, wet and annual horizontal coupons, validating the XRD findings. The elemental map emphasises the chemical compounds reported by the XRD analysis. Silicon (Si) is the most dominant element, while the rest are carbon (C), oxygen (O), sodium (Na), magnesium (Mg), aluminium (Al), calcium (Ca) and iron (Fe).

It is interesting to compare the particle sizes found in the coupons to validate the literature that reports a negative correlation between particle size and soiling impact. Fig. 17 shows the particle size distributions and frequency for the dry and wet seasons and the full year for the horizontal glass coupons. The dry season sample reports larger particles than PM10 compared to the wet season sample. The full-year sample

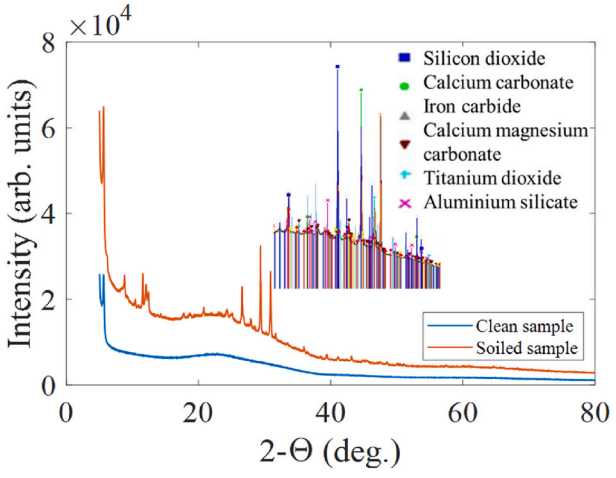

Fig. 14. XRD pattern of a clean glass coupon versus a soiled examined glass coupon. It shows peak intensity that is diffracted from the soiling particles. A snapshot of the chemical compound rays identification based on the XRD analysis is shown.

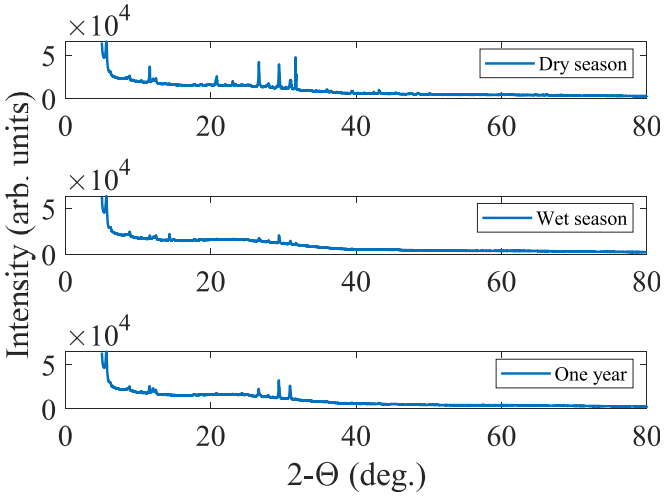

Fig. 15. XRD patterns for dry (top), wet (middle) and annual (bottom) horizontal coupons.

confirms both (the high frequency of PM10 and PM2.5), while larger particles on the dry season coupon are no longer available. The removal of larger particles is attributed to the soiling removal process that happened during the heavy rain activity of October 2021. This explains why the full-year coupon was left only with a concentration of PM10 and supports the argument that natural cleaning can only help the removal of larger particles (>10 μm). In a study conducted in Bahrain [81], which shares a similar geographical zone with the experimental site, PM10 was found to be more widespread during the dry season (August 2012), whereas PM2.5 was discovered to be more prevalent during the wet season (January 2012) [63] which aligns well with the obtained results of this study.

Since the horizontal coupons represent the worst-case conditions among the 60 samples taken throughout the study period, it is expected that those with less soiling may exhibit less particle deposition. According to light scattering theory, large particles scatter more light than small ones [82,83]. The transmittance losses during the dry season are linked with the size of particles reported in SEM images, justifying the maximum relative transmittance decrease of 66 % with the availability of large particles that align with those of previous studies. However, the moisture level supports the cementation formation during the wet season, which explains the relatively high transmittance decrease while natural cleaning is still possible. Compared to wet deposited samples, natural cleaning (the wind and gravitational influence) significantly impacts the dry deposited dust.

Overall, the SEM and XRD analysis validated the results of the experimental investigation. The findings contribute in several ways to our understanding of PV soiling in Oman and other regions that share similar environmental conditions and provide a basis for mitigation mechanisms or techniques that can be adopted in these areas.

3.4. Electrical power reduction

Soiling will affect a solar cell's power output and it is important at this point to understand quantitatively the magnitude of the electrical power losses due to soiling. When a PV module (or portion thereof) is shaded, it experiences a decrease in voltage and current, which affects its overall performance. This is because the output of PV modules is strongly related to the solar irradiance reaching the cells, such that a decrease in solar irradiance, due to partial or total shading, will influence the PV module's output. Similarly to shading, the accumulation of soiling particles can scatter, reflect and absorb the incoming sunlight and affect the light reaching the cells. Dust deposition hence reduces the short-circuit current, as this is affected by the solar illumination,

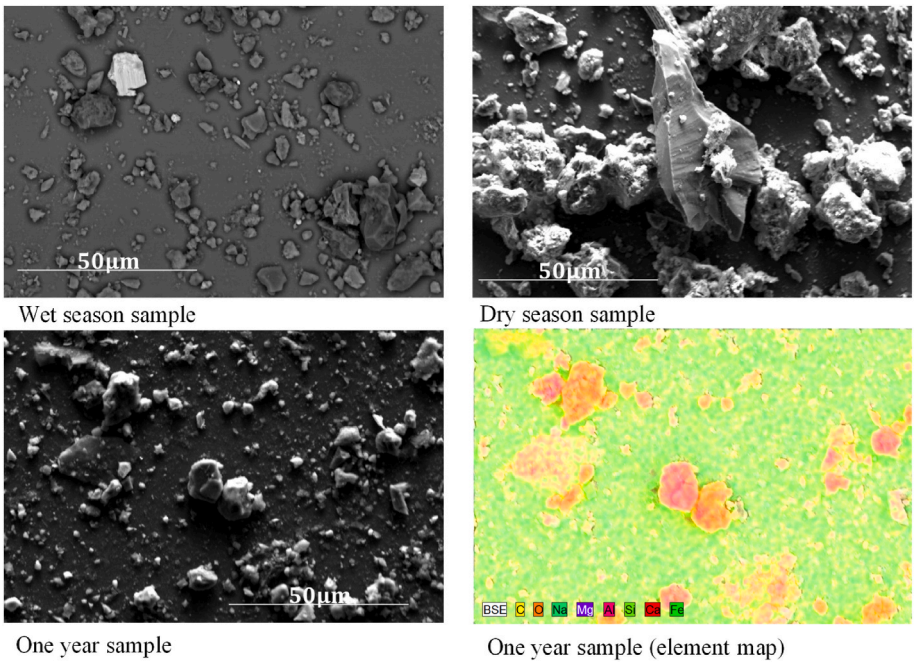

Fig. 16. SEM images of dry, wet and annual horizontal coupons with an element map of the one-year sample to represent an example of the elements found.

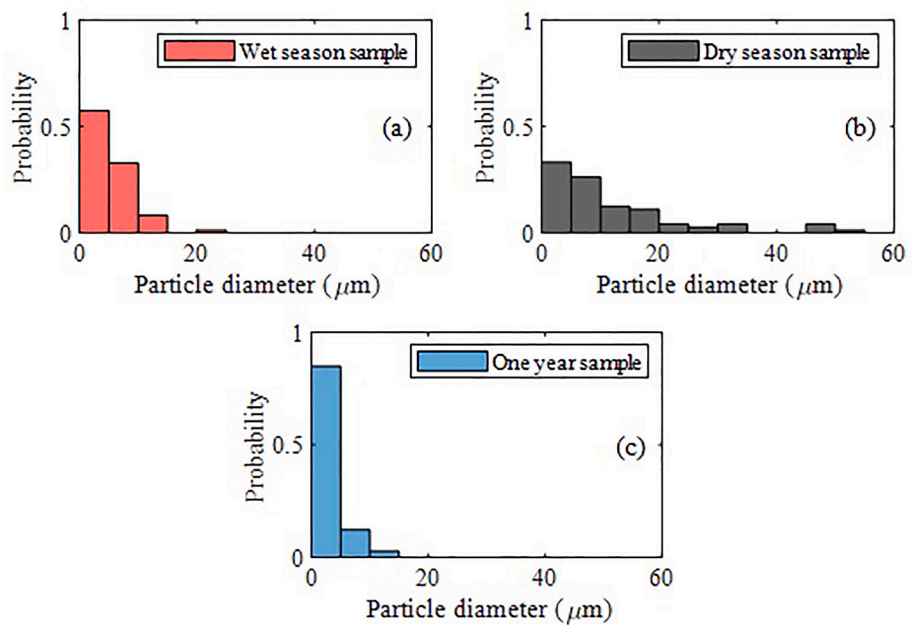

Fig. 17. Particle size distributions for: (a) wet season, (b) dry season, and (c) full-year horizontal coupons which indicate the variations in particle size across different periods.

whereas changes in temperature also affect the open-circuit voltage [63]. The quantity of dust collected on the surface of a PV module influences the overall energy provided by the module in a way that varies daily, monthly, seasonally and annually, resulting in potentially notable overall energy losses. The present analysis focuses on exploring quantitatively the effect of soiling on a PV module's power deterioration. The horizontal seasonal and full-year glass coupons were chosen for this analysis as they were the glass coupons that experienced the highest degree of soiling over the studied period and hence will have the most pronounced optical losses.

As shown in Fig. 18, the wet- and dry-season and full-year glass coupons demonstrated average (350-1100 nm) transmittance values of 34 %, 30 % and 35 %, respectively, which correspond to transmittance reductions of 62 %, 66 % and 60 % relative to the clean glass sample integrating the measured spectral transmittance of a selected soiled coupon and the spectral response of a solar cell of interest as a function of wavelength can be used to calculate the electrical power generated by the corresponding soiled cell; for example, the spectral response of the monocrystalline-silicon SunPower C60 cell is shown in Fig. 19. From this figure, we can see the direct effect of soiling on the performance of PV modules with monocrystalline solar cells. As expected, reducing the module surface's transmittance significantly decreases the spectral response, which directly affects the short circuit current (J_{sc}) of the solar cell [86]:

$$J_{SC} = \int G_{AM1.5}(\lambda)\tau_{glass}(\lambda)SR(\lambda)d\lambda, \quad (2)$$

where $G_{AM1.5}$ (λ) is the incident solar (AM1.5) spectral irradiance as a function of wavelength, τ_{glass} (λ) is the glass (and any soiling thereof) transmittance, and SR (λ) is the spectral response of the solar cell (an example of which is shown in Fig. 19).

To estimate the power loss from the PV module, the following energy balance equations are solved for the glass and PV layers in the module, considering radiative, convective and conductive heat transfer [85]: where σ is the Stefan–Boltzmann constant, T is the temperature of different layers, h_w is the convective heat transfer coefficient due to wind, R is the overall thermal resistance of different layers, α (λ) is the absorptivity of the material, $P_{el,r}$ is the reference (at 25 °C) power generated by the PV cell, and V is the applied cell voltage.

Glass :

$$\varepsilon_g\sigma\left(T_g^4 - T_{sky}^4\right) + \frac{\sigma\left(T_g^4 - T_{PV}^4\right)}{\left(\frac{1}{\varepsilon_g} + \frac{1}{\varepsilon_{PV}} - 1\right)} + h_w\left(T_g - T_a\right) + \frac{1}{R_{PV-g}}\left(T_g - T_{PV}\right) = \int \alpha_g(\lambda)\tau_g(\lambda)G_{AM1.5}(\lambda)d\lambda$$

PV :

$$\frac{\sigma\left(T_{PV}^4 - T_g^4\right)}{\left(\frac{1}{\varepsilon_g} + \frac{1}{\varepsilon_{PV}} - 1\right)} + \frac{1}{R_{PV-g}}\left(T_{PV} - T_g\right) + \frac{1}{R_{PV-a}}\left(T_{PV} - T_g\right) = \int \alpha_{PV}(\lambda)\tau_g(\lambda)G_{AM1.5}(\lambda)d\lambda - P_{el,r}[1 - \beta_{PV}(T_{PV} - 298.15)],$$

where $P_{el,r} = \max\left\{V \cdot \left[J_{sc} - J_0\left(e^{\frac{qV}{KT}} - 1\right)\right]\right\}$ (3)

From these relations, it can be observed that soiling will have two effects on the electrical performance of a PV module: (1) it will directly impact the optical transmittance and thus the solar irradiance received by the cells as described by Equation (2); while (2) also affecting the energy flows within the module, leading to changes in the temperature of the cells and, thus, the efficiency of the cells as described by Equation (3). Specifically, as the transmittance decreases due to soiling, less sunlight reaches the PV cells, also leading to a decrease in their temperature; these two effects have opposite effects on the module's electrical efficiency.

In Fig. 20, we show the decrease in the transmittance, electrical efficiency and power output of a monocrystalline Si PV module relative to an ideal (100 % transmissive) module, as evaluated from Equation (2), and the simple energy-balance model applied to PV modules in Equation (3). The relative transmittance decrease is linear, however, the relative loss of power shows a nonlinearity, for the reasons explained above. In more detail, at highly transmissive conditions (e.g., corresponding to relatively clean samples with little soiling), the loss in generated power is below what would be expected purely from the reduction in transmittance, due to the reduction in the temperature of the cells at these lower irradiance conditions. The effect of temperature accounts here for an improvement of up to 10 % of the relative drop in the electrical power and efficiency. However, as the transmittance decreases to low values (e.g., for relatively dirty samples with considerable soiling), the loss in generated power exceeds the rate at which the transmittance is reduced. This arises due to a thermal insulation effect provided by the soiling layer, which acts to trap heat within the module.

Of note is that the primary effect on the electrical performance is that of the transmittance, so these findings suggest that – at least to first order – the power output from soiled PV modules will be primarily correlated with the change in transmittance caused by the soiling. Thus, the relative transmittance reductions measured on the horizontal wet-season, dry-season and full-year samples reported earlier correspond to predicted relative reductions in electrical power generation by 62 %, 66 %, and 60 %, respectively. Based on a local tilt angle of 23°, the relative transmittance losses are estimated at around 30 % per month, resulting

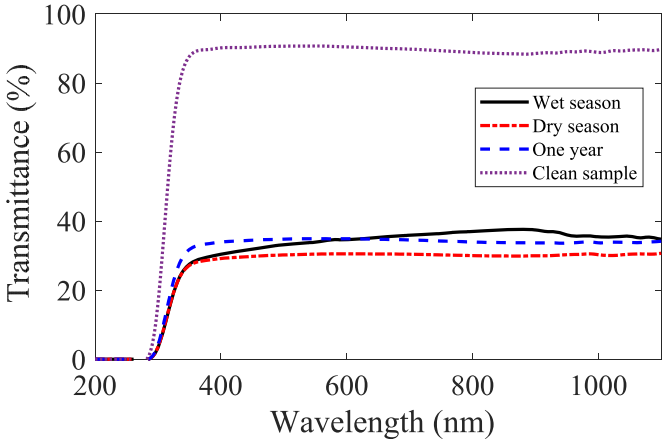

Fig. 18. Transmittance through horizontally-tilted glass coupons exposed for a full season, wet and dry, and a full year against the wavelength of the transmitted light as measured by a UV-2600 spectrophotometer. The transmittance spectrum for a clean sample is also shown.

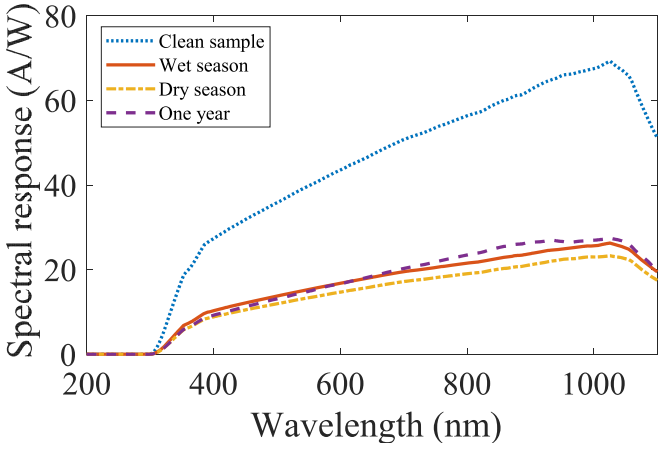

Fig. 19. Spectral response of a monocrystalline-silicon solar cell (SunPower C60) as a function of wavelength incorporating the transmittance decrease of soiled and clean coupons with separate plots for the transmittance of the coupons exposed for the duration of the wet and dry seasons and for a full year. The data for the transmittance of the coupons was obtained using a UV-2600 spectrophotometer for coupons tilted at 0°.

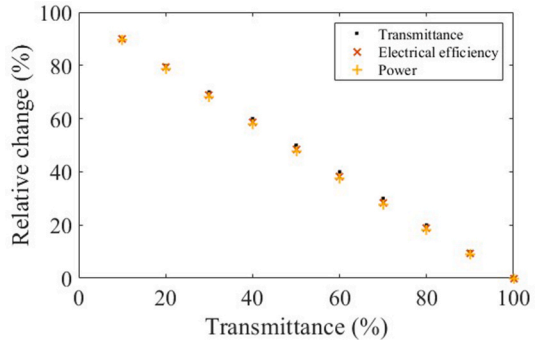

Fig. 20. Change in transmittance, electrical efficiency and power output of a monocrystalline Si PV module, relative to an ideal (100 % transmissive) module, at standard conditions as a function of transmittance.

in an equivalent relative PV power reduction of ~30 % per month at the studied location.

4. Conclusions

The experimental investigations and analyses described in this paper were designed to determine the impact of natural soiling on the transmittance of PV modules, which can in turn significantly deteriorate PV performance. The investigation critically examined the optical losses and also included material characterisation of 60 soiled glass coupons gathered over a full-year study period in 2021 in a Middle East region: Oman. Separate samples of soiling data were collected over three different time frames (at the end of each month, season, and at the end of the year). Four samples with different tilt angle positions (0°, 23°, 45°, and 90°) were collected for each time period. The findings indicate a significant monthly variation in soiling across the studied year with average relative transmittance losses of 30 % per month at the local tilt angle. Of the four tilt angles studied, horizontally-tilted coupons were found to have the highest transmittance losses. However, under high relative humidity and no-rain conditions, even the vertical coupons suffered a significant decrease in transmittance of 28 % in the vertical sample of April 2021. The horizontal wet-season, dry-season and full-year samples experienced a relative transmittance decrease of 62 %, 66 %, and 60 %, respectively, which corresponds to a relative decrease of 62 %, 66 %, and 60 % in electrical power generation perdicted for PV modules employing monocrystalline-silicon cells. A mineralogical analysis concluded that silicate materials are the most common in the studied region. It was also shown that natural cleaning due to periodic rain can eliminate the accumulation of larger particles (>10 μm), but not of smaller ones.

The soiling rate can vary greatly depending on specific, local climate conditions; consequently, accurate and local assessments and mitigation of the soiling effect are critical for maximising the energy output and efficiency of solar installations. Thus, beyond comprehensively evaluating and characterising local soiling effects, the present study lays the groundwork for future research into soiling mitigation solutions. Future work should include comprehensive explorations of seasonal soiling variations, and efforts to quantify the precise energy yield losses due to soiling, in hand with in-depth investigations of the effectiveness of current soiling mitigation practices in semi-arid environments, and investigations of more advanced strategies such as film or jet water cleaning and novel coatings. Further studies should consider the characterisation of dust particles, integrate climate data for predictive modelling, and include considerations of the sustainability of cleaning strategies. Collaborative efforts with regional researchers to create comprehensive soiling maps for the area and related assessments of environmental impacts are also essential. Finally, extending the duration of studies and comparative analyses to other climate zones will enhance our understanding of PV soiling and contribute to more efficient and sustainable solar energy utilisation in different regions.

CRediT authorship contribution statement

Tarik Alkharusi: Conceptualization, Methodology, Investigation, Validation, Visualization, Writing – original draft, Writing – review & editing. **Gan Huang:** Methodology, Writing – review & editing. **Christos N. Markides:** Conceptualization, Formal analysis, Funding acquisition, Methodology, Project administration, Resources, Supervision, Writing – review & editing.

Declaration of competing interest

The authors declare that they have no known competing financial interests or personal relationships that could have appeared to influence the work reported in this paper.

Acknowledgement

This work was supported by the UK Engineering and Physical Sciences Research Council (EPSRC) [grant number EP/R045518/1], and the Government of the Sultanate of Oman. The work was also supported by the Royal Society under an International Collaboration Award 2020 [grant number ICA\R1\201302], and UK company Solar Flow Ltd. (www.solar-flow.co.uk). The authors would like to thank Chandan Pandey, Andreas Olympios and Benedict Winchester from the Clean Energy Processes (CEP) Laboratory, and Ned Ekins-Daukes from the University of New South Wales for their useful contributions. Data supporting this publication can be obtained on request from cep-lab@imperial.ac.uk. For the purpose of Open Access, the authors have applied a CC BY public copyright licence to any Author Accepted Manuscript version arising from this submission.

References

[1] A. Olympios, M. Aunedi, M. Mersch, A. Krishnaswamy, et al., Delivering net-zero carbon heat: technoeconomic and whole-system comparisons of domestic electricity- and hydrogen-driven technologies in the UK, Energy Convers. Manag. 262 (2022), 115649, https://doi.org/10.1016/J.ENCONMAN.2022.115649.
[2] Solar Power Europe, Global Market Outlook for Solar Power 2022-2026, 2022. (Accessed 7 June 2022).
[3] International Renewable Energy Agency, Global Energy Transformation: A Roadmap to 2050, 2019. (Accessed 15 October 2020).
[4] International Energy Agency, Renewables Information: Overview, 2020. (Accessed 15 October 2020).
[5] G. Huang, C.N. Markides, Spectral-splitting hybrid PV-thermal (PV-T) solar collectors employing semi-transparent solar cells as optical filters, Energy Convers. Manag. (2021) 248, https://doi.org/10.1016/J.ENCONMAN.2021.114776.
[6] H. Liang, R. Su, W. Huang, Z. Cheng, et al., A novel spectral beam splitting photovoltaic/thermal hybrid system based on semi-transparent solar cell with serrated groove structure for co-generation of electricity and high-grade thermal energy, Energy Convers. Manag. (2022) 252, https://doi.org/10.1016/J.ENCONMAN.2021.115049.
[7] R. Madurai Elavarasan, V. Mudgal, L. Selvamanohar, K. Wang, et al., Pathways toward high-efficiency solar photovoltaic thermal management for electrical, thermal and combined generation applications: a critical review, Energy Convers. Manag. 255 (2022), 115278, https://doi.org/10.1016/J.ENCONMAN.2022.115278.
[8] M. Herrando, K. Wang, G. Huang, T. Otanicar, et al., A review of solar hybrid photovoltaic-thermal (PV-T) collectors and systems, Prog. Energy Combust. Sci. 97 (2023), 101072, https://doi.org/10.1016/J.PECS.2023.101072.
[9] M. Herrando, A. Ramos, J. Freeman, I. Zabalza, C.N. Markides, Technoeconomic modelling and optimisation of solar combined heat and power systems based on flat-box PVT collectors for domestic applications, Energy Convers. Manag. 175 (2018) 67–85, https://doi.org/10.1016/J.ENCONMAN.2018.07.045.
[10] A. Ramos, M. Chatzopoulou, I. Guarracino, J. Freeman, et al., Hybrid photovoltaic-thermal solar systems for combined heating, cooling and power provision in the urban environment, Energy Convers. Manag. 150 (2017) 838–850, https://doi.org/10.1016/J.ENCONMAN.2017.03.024.
[11] S. Navakrishnan, E. Vengadesan, R. Senthil, S. Dhanalakshmi, An experimental study on simultaneous electricity and heat production from solar PV with thermal energy storage, Energy Convers. Manag. 245 (2021), 114614, https://doi.org/10.1016/J.ENCONMAN.2021.114614.

[12] W. He, G. Huang, C.N. Markides, Synergies and potential of hybrid solar photovoltaic-thermal desalination technologies, Desalination (2023) 552, https://doi.org/10.1016/J.DESAL.2023.116424.
[13] S. Shoeibi, M. Saemian, M. Khiadani, H. Kargarsharifabad, et al., Influence of PV/T waste heat on water productivity and electricity generation of solar stills using heat pipes and thermoelectric generator: an experimental study and environmental analysis, Energy Convers. Manag. 276 (2023), 116504, https://doi.org/10.1016/J.ENCONMAN.2022.116504.
[14] G. Huang, J. Xu, C.N. Markides, High-efficiency bio-inspired hybrid multi-generation photovoltaic leaf, Nat. Commun. 14 (1) (2023) 3344, https://doi.org/10.1038/S41467-023-38984-7.
[15] P.K. Enaganti, A. Bhattacharjee, A. Ghosh, Experimental investigations for dust build-up on low-iron glass exterior and its effects on the performance of solar PV systems, Energy 239 (2022), 122213, https://doi.org/10.1016/J.ENERGY.2021.122213.
[16] B. Laarabi, Y. El Baqqal, A. Dahrouch, A. Barhdadi, Deep analysis of soiling effect on glass transmittance of PV modules in seven sites in Morocco, Energy 213 (2020), 118811, https://doi.org/10.1016/J.ENERGY.2020.118811.
[17] K. Hasan, S. Yousuf, M. Tushar, B.K. Das, et al., Effects of different environmental and operational factors on the PV performance: a comprehensive review, Energy Sci. Eng. 10 (2) (2022) 656–675, https://doi.org/10.1002/ESE3.1043.
[18] H. Zitouni, A. Azouzoute, C. Hajjaj, M. Ydrissiet, et al., Experimental investigation and modeling of photovoltaic soiling loss as a function of environmental variables: a case study of semi-arid climate, Sol. Energy Mater. Sol. Cells 221 (2021), 110874, https://doi.org/10.1016/J.SOLMAT.2020.110874.
[19] J. Polo, N. Chivelet, C. Sanz-Saiz, J. Montesinos, et al., Modeling soiling losses for rooftop PV systems in suburban areas with nearby forest in Madrid, Renew. Energy 178 (2021) 420–428, https://doi.org/10.1016/J.RENENE.2021.06.085.
[20] Y. Chanchangi, A. Roy, A. Ghosh, S. Sundaram, et al., In-situ assessment of photovoltaic soiling mitigation techniques in northern Nigeria, Energy Convers. Manag. (2021) 244, https://doi.org/10.1016/J.ENCONMAN.2021.114442.
[21] K. Chiteka, R. Arora, S. Sridhara, C.C. Enweremadu, Influence of irradiance incidence angle and installation configuration on the deposition of dust and dust-shading of a photovoltaic array, Energy 216 (2021), 119289, https://doi.org/10.1016/J.ENERGY.2020.119289.
[22] A. Pan, H. Lu, L.Z. Zhang, Experimental investigation of dust deposition reduction on solar cell covering glass by different self-cleaning coatings, Energy 181 (2019) 645–653, https://doi.org/10.1016/J.ENERGY.2019.05.223.
[23] K.K. Ilse, B.W. Figgis, M. Werner, V. Naumann, et al., Comprehensive analysis of soiling and cementation processes on PV modules in Qatar, Sol. Energy Mater. Sol. Cells 186 (2018) 309–323, https://doi.org/10.1016/J.SOLMAT.2018.06.051.
[24] A. Wang, Y. Xuan, Close examination of localised hot spots within photovoltaic modules, Energy Convers. Manag. (2021) 234, https://doi.org/10.1016/J.ENCONMAN.2021.113959.
[25] K. Ilse, L. Micheli, B.W. Figgis, K. Lang, et al., Techno-Economic assessment of soiling losses and mitigation strategies for solar power generation, Joule 3 (10) (2019) 2303–2321, https://doi.org/10.1016/J.JOULE.2019.08.019.
[26] M. Bergin, C. Ghoroi, D. Dixit, J.J. Schauer, et al., Large reductions in solar energy production due to dust and particulate air pollution, Environ. Sci. Technol. Lett. 4 (8) (2017) 339–344, https://doi.org/10.1021/ACS.ESTLETT.7B00197.
[27] International Energy Agency, Renewables Information Analysis, 2019. (Accessed 15 October 2020).
[28] X. Li, F. Wagner, W. Peng, J. Yang, et al., Reduction of solar photovoltaic resources due to air pollution in China, PNAS USA 114 (45) (2017) 11867–11872, https://doi.org/10.1073/PNAS.1711462114.
[29] X. Li, D.L. Mauzerall, M.H. Bergin, Global reduction of solar power generation efficiency due to aerosols and panel soiling, Nat. Sustain. 3 (9) (2020) 720–727, https://doi.org/10.1038/S41893-020-0553-2.
[30] S. Ghazi, A. Sayigh, K. Ip, Dust effect on flat surfaces – a review paper, Renew. Sustain. Energy Rev. 33 (2014) 742–751, https://doi.org/10.1016/J.RSER.2014.02.016.
[31] O.A. Choobari, P. Zawar-Reza, A. Sturman, The global distribution of mineral dust and its impacts on the climate system: a review, Atmos. Res. 138 (2014) 152–165, https://doi.org/10.1016/J.ATMOSRES.2013.11.007.
[32] R. Conceição, I. Vázquez, L. Fialho, D. García, Soiling and rainfall effect on PV technology in rural Southern Europe, Renew. Energy 156 (2020) 743–747, https://doi.org/10.1016/J.RENENE.2020.04.119.
[33] M.J. Adinoyi, S.A.M. Said, Effect of dust accumulation on the power outputs of solar photovoltaic modules, Renew. Energy 60 (2013) 633–636, https://doi.org/10.1016/J.RENENE.2013.06.014.
[34] Y. Chanchangi, A. Ghosh, H. Baig, S. Sundaram, et al., Soiling on PV performance influenced by weather parameters in Northern Nigeria, Renew. Energy 180 (2021) 874–892, https://doi.org/10.1016/J.RENENE.2021.08.090.
[35] Y. Chanchangi, A. Ghosh, L. Micheli, F. Fernández, et al., Soiling mapping through optical losses for Nigeria, Renew. Energy 197 (2022) 995–1008, https://doi.org/10.1016/J.RENENE.2022.07.019.
[36] P. Enaganti, A. Bhattacharjee, A. Ghosh, Experimental investigations for dust build-up on low-iron glass exterior and its effects on the performance of solar PV systems, Energy 239 (2022) 122–213, https://doi.org/10.1016/J.ENERGY.2021.122213.
[37] M. Abdolzadeh, R. Nikkhah, Experimental study of dust deposition settled over tilted PV modules fixed in different directions in the southeast of Iran, Environ. Sci. Pollut. Res. 26 (2019) 31478–31490, https://doi.org/10.1007/S11356-019-06246-Z.
[38] A. Gholami, I. Khazaee, S. Eslami, M. Zandi, et al., Experimental investigation of dust deposition effects on photovoltaic output performance, Sol. Energy 159 (2018) 346–352, https://doi.org/10.1016/J.SOLENER.2017.11.010.
[39] H. Elminir, A.E. Ghitas, R.H. Hamid, F. El-Hussainy, et al., Effect of dust on the transparent cover of solar collectors, Energy Convers. Manag. 47 (2006) 3192–3203, https://doi.org/10.1016/J.ENCONMAN.2006.02.014.
[40] R. Xu, K. Ni, Y. Hu, J. Si, et al., Analysis of the optimum tilt angle for a soiled PV panel, Energy Convers. Manag. 148 (2017) 100–109, https://doi.org/10.1016/J.ENCONMAN.2017.05.058.
[41] A. El-Nashar, Seasonal effect of dust deposition on a field of evacuated tube collectors on the performance of a solar desalination plant, Desalination 239 (2009) 66–81, https://doi.org/10.1016/J.DESAL.2008.03.007.
[42] A. Ullah, H. Imran, Z. Maqsood, N. Butt, Investigation of optimal tilt angles and effects of soiling on PV energy production in Pakistan, Renew. Energy 139 (2019) 830–843, https://doi.org/10.1016/J.RENENE.2019.02.114.
[43] A. Ullah, A. Amin, T. Haider, M. Saleem, et al., Investigation of soiling effects, dust chemistry and optimum cleaning schedule for PV modules in Lahore, Pakistan, Renew. Energy 150 (2020) 456–468, https://doi.org/10.1016/J.RENENE.2019.12.090.
[44] M. Mazumder, R. Sharma, A. Biris, J. Zhang, et al., Self-cleaning transparent dust shields for protecting solar panels and other devices, Part. Sci. Technol. 25 (1) (2007) 5–20, https://doi.org/10.1080/02726350601146341.
[45] D. Dehshiri, B. Firoozabadi, Dust cycle, soiling effect and optimum cleaning schedule for PV modules in Iran: a long-term multi-criteria analysis, Energy Convers. Manag. 286 (2023), 117084, https://doi.org/10.1016/J.ENCONMAN.2023.117084.
[46] M. Abraim, M. Salihi, O. El Alani, et al., Techno-economic assessment of soiling losses in CSP and PV solar power plants: a case study for the semi-arid climate of Morocco, Energy Convers. Manag. 270 (2022), 116285, https://doi.org/10.1016/J.ENCONMAN.2022.116285.
[47] Y. Chanchangi, A. Ghosh, S. Sundaram, T.K. Mallick, Dust and PV performance in Nigeria: a review, Renew. Sustain. Energy Rev. 121 (2020), 109704, https://doi.org/10.1016/J.RSER.2020.109704.
[48] X. Liu, S. Yue, L. Lu, J. Li, Investigation of the dust scaling behaviour on solar photovoltaic panels, J. Clean. Prod. 295 (2021), 126391, https://doi.org/10.1016/J.JCLEPRO.2021.126391.
[49] T. Sarver, A. Al-Qaraghuli, L.L. Kazmerski, A comprehensive review of the impact of dust on the use of solar energy: history, investigations, results, literature, and mitigation approaches, Renew. Sustain. Energy Rev. 22 (2013) 698–733, https://doi.org/10.1016/J.RSER.2012.12.065.
[50] E. Urrejola, J. Antonanzas, P. Ayala, M. Salgado, et al., Effect of soiling and sunlight exposure on the performance ratio of photovoltaic technologies in Santiago, Chile, Energy Convers. Manag. 114 (2016) 338–347, https://doi.org/10.1016/J.ENCONMAN.2016.02.016.
[51] M. Rahman, J. Selvaraj, N. Rahim, M. Hasanuzzaman, Global modern monitoring systems for PV based power generation: a review, Renew. Sustain. Energy Rev. 82 (2018) 4142–4158, https://doi.org/10.1016/J.RSER.2017.10.111.
[52] M. Abraim, M. El Ydrissi, H. Ghennioui, PVSMS: a system for quantifying soiling effects and optimising cleaning schedule in PV solar plants, Energy Convers. Manag. 284 (2023), 116978, https://doi.org/10.1016/J.ENCONMAN.2023.116978.
[53] K. Burrows, V. Fthenakis, Glass needs for a growing photovoltaics industry, Sol. Energy Mater. Sol. Cell. 132 (2015) 455–459, https://doi.org/10.1016/J.SOLMAT.2014.09.028.
[54] Y.N. Chanchangi, A. Ghosh, S. Sundaram, T.K. Mallick, Angular dependencies of soiling loss on photovoltaic performance in Nigeria, Sol. Energy 225 (2021) 108–121, https://doi.org/10.1016/J.SOLENER.2021.07.001.
[55] A. Azouzoute, C. Hajjaj, H. Zitouni, M. Ydrissiet, et al., Modeling and experimental investigation of dust effect on glass cover PV module with fixed and tracking system under semi-arid climate, Sol. Energy Mater. Sol. Cells 230 (2021), 111219, https://doi.org/10.1016/J.SOLMAT.2021.111219.
[56] D. Olivares, P. Ferrada, A. Marzo, J. Llanos, et al., Microstructural analysis of the PV module cementation process at the solar platform of the atacama desert, Sol. Energy Mater. Sol. Cells 227 (2021), 111109, https://doi.org/10.1016/J.SOLMAT.2021.111109.
[57] H. Ahmed, S. Al-Brashdi, Forecasting Techniques for Seedable Storms over the Western Hajar Mountains in the Sultanate of Oman, Department of geography, university of Pretoria, 2007.
[58] Global solar atlas, Available online at: https://globalsolaratlas.info/map?c=23.584126,58.436279, 7&s=23.593879,58.426902&m=site.
[59] M.Z. Khan, A. Ghaffar, M.A. Bahattab, et al., Outdoor performance of anti-soiling coatings in various climates of Saudi Arabia, Sol. Energy Mater. Sol. Cells 235 (2022), 111470, https://doi.org/10.1016/J.SOLMAT.2021.111470.
[60] M.R. Maghami, H. Hizam, C. Gomes, M. Radzi, et al., Power loss due to soiling on solar panel: a review, Renew. Sustain. Energy Rev. 59 (2016) 1307–1316, https://doi.org/10.1016/J.RSER.2016.01.044.
[61] E. Fares, M. Buffiere, B. Figgis, Y. Haik, et al., Soiling of photovoltaic panels in the Gulf Cooperation Council countries and mitigation strategies, Sol. Energy Mater. Sol. Cells (2021) 231, https://doi.org/10.1016/J.SOLMAT.2021.111303.
[62] Civil Aviation Authority. Metrological data; available online at https://www.caa.gov.om/caadicorates/directorate-general-of-meteorology.
[63] Y. Chanchangi, A. Ghosh, S. Sundaram, T. Mallick, An analytical indoor experimental study on the effect of soiling on PV, focusing on dust properties and PV surface material, Sol. Energy 203 (2020) 46–68, https://doi.org/10.1016/J.SOLENER.2020.03.089.
[64] B. Henson, J. Masters, Shaheen pushes onshore as first tropical cyclone on record in far north Oman, Yale Climate Connections, available at: https://yaleclimateconnections.org/2021/10/shaheen-pushes-onshore-as-first-tropical-cyclone-on-record-in-far-north-oman, 2021 (Accessed 1 May 2023).

[65] T. Salamah, A. Ramahi, K. Alamara, Effect of dust and methods of cleaning on the performance of solar PV module for different climate regions: comprehensive review, Sci. Total Environ. 827 (2022), 154050, https://doi.org/10.1016/J.SCITOTENV.2022.154050.
[66] S. Toth, M. Muller, D. Miller, Soiling and cleaning: initial observations from 5-year photovoltaic glass coating durability study, Sol. Energy Mater. Sol. Cell. 185 (2018) 375–384, https://doi.org/10.1016/J.SOLMAT.2018.05.039.
[67] B. Figgis, G. Scabbia, B. Aissa, Condensation as a predictor of PV soiling, Sol. Energy 238 (2022) 30–38, https://doi.org/10.1016/J.SOLENER.2022.04.025.
[68] B. Figgis, A. Nouviaire, Y. Wubulikasimu, et al., Investigation of factors affecting condensation on soiled PV modules, Sol. Energy 159 (2018) 488–500, https://doi.org/10.1016/J.SOLENER.2017.10.089.
[69] B. Yilbas, H. Ali, M. Khaled, N. Al-Aqeeli, et al., Influence of dust and mud on the optical, chemical and mechanical properties of a pv protective glass, Sci. Rep. 5 (1) (2015) 1–12, https://doi.org/10.1038/SREP15833.
[70] R. Conceição, H.G. Silva, M. Collares-Pereira, CSP mirror soiling characterisation and modeling, Sol. Energy Mater. Sol. Cells 185 (2018) 233–239, https://doi.org/10.1016/J.SOLMAT.2018.05.035.
[71] M. Hossain, A. Ali, B. Bermudez, B. Figgis, et al., Anti-soiling coatings for enhancement of PV panel performance in desert environment: a critical review and market overview, Mater. 15 (20) (2022), https://doi.org/10.3390/MA15207139.
[72] S. Said, H. Walwil, Fundamental studies on dust fouling effects on PV module performance, Sol. Energy 107 (2014) 328–337, https://doi.org/10.1016/J.SOLENER.2014.05.048.
[73] W. Zhao, Y. Lv, Q. Zhou, W. Yan, Investigation on particle deposition criterion and dust accumulation impact on solar PV module performance, Energy (2021) 233, https://doi.org/10.1016/J.ENERGY.2021.121240.
[74] A. Gholami, A. Saboonchi, A. Alemrajabi, Experimental study of factors affecting dust accumulation and their effects on the transmission coefficient of glass for solar applications, Renew. Energy 112 (2017) 466–473, https://doi.org/10.1016/J.RENENE.2017.05.050.
[75] S. Pulipaka, R. Kumar, Analysis of irradiance losses on a soiled photovoltaic panel using contours, Energy Convers. Manag. 115 (2016) 327–336, https://doi.org/10.1016/J.ENCONMAN.2016.02.068.
[76] Z. Jian, W. HelING, The physical meanings of 5 basic parameters for an X-ray diffraction peak and their application, Chin. J. Geochem. 22 (1) (2003) 38–44, https://doi.org/10.1007/BF02831544.
[77] H. Al-Shidi, H. Al-Reasi, H. Sulaiman, Heavy metals levels in road dust from Muscat, Oman: relationship with traffic volumes, and ecological and health risk assessments, Environ. Res. Public Health 32 (2) (2020) 264–276, https://doi.org/10.1080/09603123.2020.1751806.
[78] A. Farahat, Air pollution in the Arabian Peninsula (Saudi Arabia, the United Arab Emirates, Kuwait, Qatar, Bahrain, and Oman): causes, effects, and aerosol categorisation, Arabian J. Geosci. 196 (9) (2016), https://doi.org/10.1007/S12517-015-2203-Y.
[79] B. Jiu, W. Huang, J. Shi, M. He, Growth mechanism of siliceous cement in tight sandstone and its influence on reservoir physical properties, Energies 11 (11) (2018) 3133, https://doi.org/10.3390/EN11113133.
[80] L.D. Norton, Micromorphology of silica cementation in soils, Dev. Soil Sci. 22 (C) (1993) 811–824, https://doi.org/10.1016/S0166-2481(08)70465-3.
[81] M.S. Jassim, G. Coskuner, Assessment of spatial variations of particulate matter (PM10 and PM2.5) in Bahrain identified by air quality index (AQI), Arabian J. Geosci. 10 (1) (2017) 1–14, https://doi.org/10.1007/S12517-016-2808-9/FIGURES/17.
[82] Horiba Ltd, Light scattering theory-laser Diffraction (static light scattering), Horiba Documents (2007).
[83] R. Xu, Light scattering: a review of particle characterisation applications, Particuology 18 (2015) 11–21, https://doi.org/10.1016/J.PARTIC.2014.05.002.
[84] F. Giovannetti, S. Föste, N. Ehrmann, G. Rockendorf, High transmittance, low emissivity glass covers for flat plate collectors: applications and performance, Sol. Energy 104 (2014) 52–59, https://doi.org/10.1016/J.SOLENER.2013.10.006.
[85] M. Herrando, C.N. Markides, K. Hellgardt, A UK-based assessment of hybrid PV and solar-thermal systems for domestic heating and power: system performance, Appl. Energy 122 (2014) 288–309, https://doi.org/10.1016/J.APENERGY.2014.01.061.
[86] G. Huang, K. Wang, C.N. Markides, Efficiency limits of concentrating spectral-splitting hybrid photovoltaic-thermal (PV-T) solar collectors and systems, Light Sci. Appl. 10 (2021) 28, doi:10.1038/S41377-021-00465-1.